



Tailoring the performance of bamboo filler reinforced epoxy composite: insights into fracture properties and fracture mechanism

Rahul Kumar¹ · Kaushik Kumar² · Sumit Bhowmik¹  · Gautam Sarkhel³

Received: 21 April 2018 / Accepted: 25 January 2019 / Published online: 1 February 2019
© The Polymer Society, Taipei 2019

Abstract

Due to the graded micro-structure and high specific strength-stiffness, bamboo micro fillers are systematically utilized in reinforcing different thermoset and thermoplastic polymers as replacement of conventional glass and carbon fillers. In this work, micro-size bamboo particle fillers are reinforced in ‘specific grade’ thermoset epoxy matrix and its fracture properties has been evaluated by following linear elastic fracture mechanics. To enhance its compatibility with the polymer matrix and to reduce the hydrophilicity, the bamboo micro fillers are surface modified through alkaline treatment. The extent of surface modification and removal of lower weight polymers from filler surface are examined and established by Fourier transform infrared (FTIR) spectroscopy, X-ray diffraction analysis and thermogravimetric analysis. The fracture properties of bamboo-epoxy composite material are observed to be increasing with the addition of bamboo fillers and the maximum value of fracture toughness is $0.678 \text{ MPa}\cdot\text{m}^{0.5}$ which is 32% higher than the same for neat epoxy samples. In addition, the mechanisms of notch initiated fracture propagation have also been explained for the understanding of stress singularity present at the preexisted crack tip.

Keywords Bamboo · Particle filler · Epoxy matrix · Fracture toughness · Binary phase

Introduction

Emergent ecological attentiveness throughout the world has elicited a paradigm shift towards designing materials well-suited to the environment. Perpetually growing demand for lighter in addition to stiffer material has resulted in the large-scale industrial production and commercial use of petroleum-based plastic materials [1–3]. Nonetheless, the grave concern regarding the environmental pollution and ecological misbalance due to their disposal at the end of the life-cycle prompted the research interests towards the development of environment friendly reinforced polymer composite materials [4–6]. In this context, the reinforcements derived from natural lignocellulosic biomass has

gained significant attention for powerful feedstock as replacement of petroleum-based fossil materials in the manufacturing of polymer composites. Amongst the numerous lignocellulosic-based reinforcements, bamboo (a class of perennial flowering plants) has several intrinsic benefits like faster growth cycle, lighter weight and abundant availability. The bamboo fibre is also known as ‘natural glass fibre’ due to its macroscopic graded structure and high specific strength to stiffness ratio [7, 8]. Regardless of aforementioned benefits, certain inherent drawbacks are hydrophilic and polar nature that lead to incompatibility and poor adhesion between reinforcing fibre and polymer matrix, eventually resulting in inferior mechanical properties. However, adhesion issues can be overcome by modifying fibre surface through any chemical or physical treatment process. Several chemical treatment processes like alkaline treatment, silane treatment to name few are available and among this, alkali treatment using aqueous NaOH solution is simple and effective [9, 10]. In recent times, numerous research works have been conducted on bamboo fibre reinforced polymer composites [11–15] but very few works are carried out on filler form of reinforcement of bamboo-based lignocellulosic biomass [16, 17].

The micro-sized particle fillers are presently considered as potential reinforcing material owing to its reinforcing

✉ Sumit Bhowmik
bhowmiksumit04@yahoo.co.in

¹ Department of Mechanical Engineering, National Institute of Technology, Silchar, India

² Department of Mechanical Engineering, Birla Institute of Technology, Mesra, India

³ Department of Chemical Engineering and Technology, Birla Institute of Technology, Mesra, India

capabilities along with improving properties of polymeric resins. The micron and submicron size range fillers are found to be superior to their nano counterpart because diminished distances between fillers lead to better distribution and continuous phase preferential immersion to the phase with better surface affinity and pinned the phase structure due to low mobility of the filler particles [18, 19]. Moreover, the phase separation (a critical factor in decisive mechanical properties) is usually more prominent in case of inclusion of micro size fillers in polymer blends [20]. Recently, a work on size fractionated bio-carbon reinforced poly(lactic acid) (PLA) based blend has demonstrated the good mechanical properties and better dispersion of filler particles in the polymer matrix for a particle size range of 20–75 μm [21]. Keeping in mind the aforesaid facts, the present research work is defined to investigate the effect of bamboo fillers of ‘particular size range’ on the dispersion and fracture properties of ‘specific grade’ epoxy composite. Additionally, the bamboo filler is chemically treated before reinforcement with aqueous NaOH solution to remove waxy layers present on the surface and improve the mechanical interlocking with the matrix. The focus of the present work is to tailor make the fracture properties (through a proper interaction of filler with blending matrix) that play a key role in determining its potential application for a wide range of products. The mechanisms of notch initiated fracture initiation and propagation has also been explained in a lucid manner for the deeper understanding of stress singularity present at the preexisted crack tip. The findings in this work will shed light on the toughening behaviour of epoxy composites with bamboo micro particle filler reinforcement and subsequent opportunities of this material as superior green composites.

Materials and experimental details

Matrix and reinforcing material

The standard ‘adhesive grade’ epoxy resin AW 106 and corresponding hardener HV 953IN procured from Huntsman India, is used as matrix material. The number average molecular weight of the corresponding epoxy resin lies between 700 and 1100. The chemical composition of resin and hardener is bisphenol F-epoxy resin and 1,8-p-menthenediamine respectively [22]. The molecular structure of the resin and hardener is shown in Fig. 1a, b respectively. The specific gravity of hardener and resin are 0.92 and 1.17 g/cc respectively whereas resin-hardener mixture viscosity is 45,000 cP at room temperature. The molar ratio of resin and hardener used in the present work is 3.38:1.

The bamboo culms are received from local resources and as-received bamboo culms are soaked in water for some time

before subjected to extraction of the fibrous parts from it. The extracted fibrous parts are dried and chopped to obtain bamboo fillers. Then the bamboo fillers are pulverized in powder form with a planetary ball mill. The mechanical milling through steel balls has produced various shapes of particles as the fracture of particles took place by abrasion, impact and cleavage [23]. To obtain the required particle size range, the powdered bamboo filler is sieved through a set of sieves placed in the descending order of their fineness as shown in Fig. 2a. Afterward, the bamboo filler with the particle size less than 75 μm is collected from the base container and subjected to washing and oven drying. The stacking of sieves and particle size distribution (in %) are shown in Fig. 2a, b respectively. The optical micrograph of the dried filler at two different magnification are shown in Fig. 3a. The elemental distribution of the bamboo filler is depicted in Fig. 3b as energy dispersive spectroscopy (EDS).

The EDS analysis principally revealed the presence of oxygen and carbon atoms in the bio-filler molecular structure. The carbon and oxygen atoms present in filler molecules are in form of carbonyl groups, hydroxyl groups and carboxyl groups as observed in FTIR spectra. The corresponding weight % of carbon and oxygen elements are 50.46 and 48.77 respectively.

Chemical treatment and composite fabrication

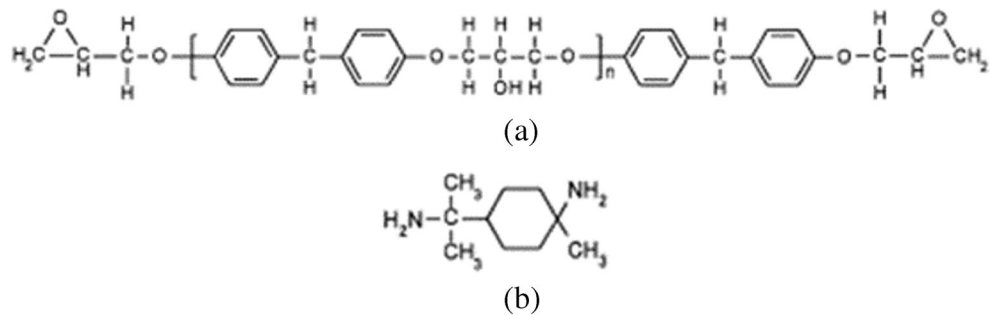
The bamboo particle fillers are subjected to alkali treatment through 5% (w/v) NaOH solution and then heated to 50 °C, maintained at the same temperature for 8 h. Initially 5 g of NaOH pallet has been dispersed in 100 ml of distilled water to prepare the required aqueous basic solution and after some time 8 g of bamboo filler is added to form a homogeneous suspension. This solution is stirred at 870 rpm and 50 °C for 8 h to complete the reaction. Later on, the soaked fillers are washed several times with distilled water and acetone until neutral. Subsequently, the washed fillers are oven dried at 70 °C for overnight and sealed in an airtight polyethene bag until needed [24]. The reaction mechanism for this thermodynamically favored chemical reaction is shown in Fig. 4. The percentage removal of lignin and other lower weight polymers can be calculated by following Eq. 1. The weight loss is measured primarily after 8 h of alkali treatment and corresponding value (in %) are shown in Table 1.

$$P_{WL} = \frac{W_B - W_A}{W_B} \times 100 \quad (1)$$

Where P_{WL} —% Weight loss, W_B —Weight of filler before treatment, W_A — Weight of filler after treatment.

Binary composites consisting of thermoset epoxy and bamboo filler (weight % of 2.5, 5, 7.5, 10 and 12.5) are prepared by hand layup technique. Initially, the resin and hardener are blended in a weight ratio of 10:8 (as recommended by manufacturer)

Fig. 1 a Molecular structure of epoxy resin and amine based hardener



and agitated for 5–6 min with the help of overhead stirrer. Next, the required amount of bamboo filler is dispersed in the resin-hardener mixture and again stirred for 10–15 min at 100 rpm under mechanical stirrer. The entire mixture is then degassed in 0.1 Torr vacuum desiccator. Subsequently, the whole mixture is gradually poured in the silicon rubber mould of required dimension according to the ASTM standard (ASTM D-5045-14) and a roller is passed over it to remove the excess material from mould and air trapped during pouring. After the whole mould set up is left at room temperature for 12 h and then in a hot air oven at 70 °C for post curing of samples. The employed post curing time is 2 h. Later on, the composite specimens are taken out and subjected to fracture toughness test.

Experimentation

Characterization of bamboo filler

The effect of alkali treatment on untreated bamboo filler is assessed by Fourier transform infrared spectroscopy (FTIR), X-ray diffraction (XRD) and thermogravimetric analysis (TGA).

To analyze the presence of the functional group in the sample, the structural analysis of treated and untreated filler is carried out using Fourier transform infrared spectroscopy (FTIR) in transmission mode with spectra recorded in the transmittance range of 3900–450 cm⁻¹ having resolution scans of 2 cm⁻¹. The sample is prepared in pallet form with dried and ground bamboo filler mixed with potassium bromide (KBr) powder. The weight ratio of bamboo filler and KBr powder used for the preparation of solid pallet is 1:150 (2 mg of bamboo filler, 300 mg of KBr powder). The number of scans used for the FTIR experiment in the present research work is 65. The average particle size of bamboo filler is around 5–6 μm after grinding process and the same particle size is used in the sample preparation prior to the FTIR experiment.

The phase and crystallinity analysis of alkali-treated and untreated bamboo filler material are carried out using wide-angle Brucker D8 Advance X-ray diffractometer (XRD) operated at 30 kV/15 mA. The diffraction intensities are recorded in a 2θ scale from 10° to 45° at a speed of 2°/min in steps of 0.05° to show the clear distinction between the spectra of treated and untreated filler. The wavelength of X-ray source for the diffraction analysis is 1.54060 Å.

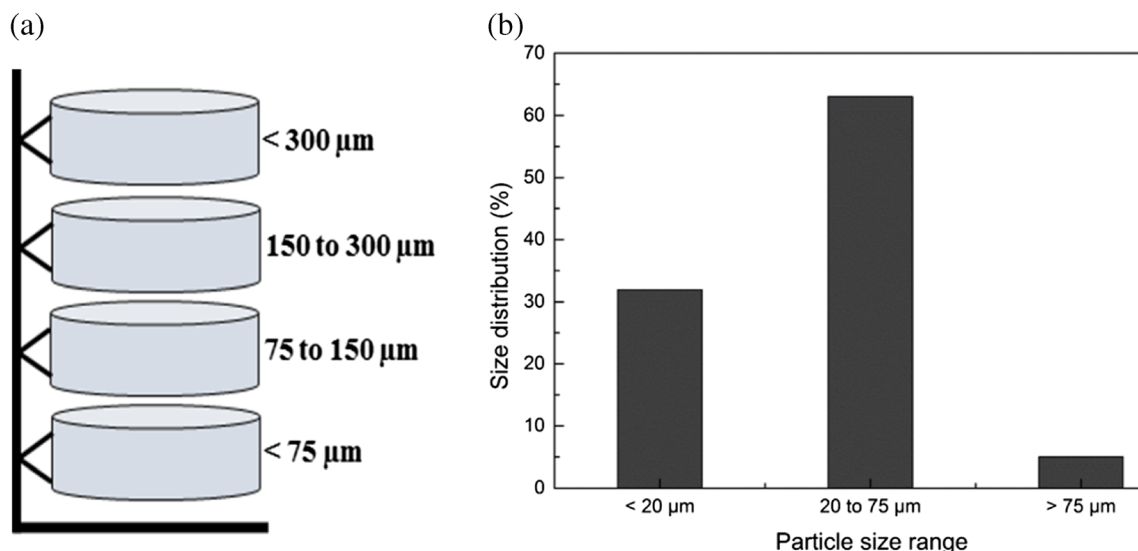
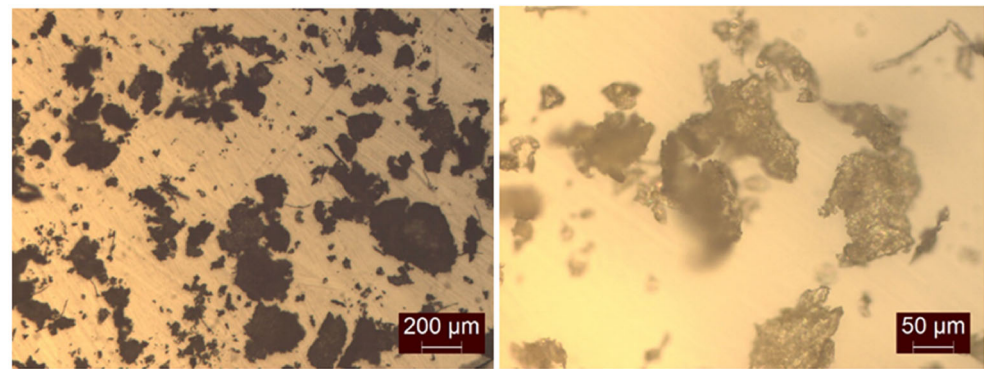
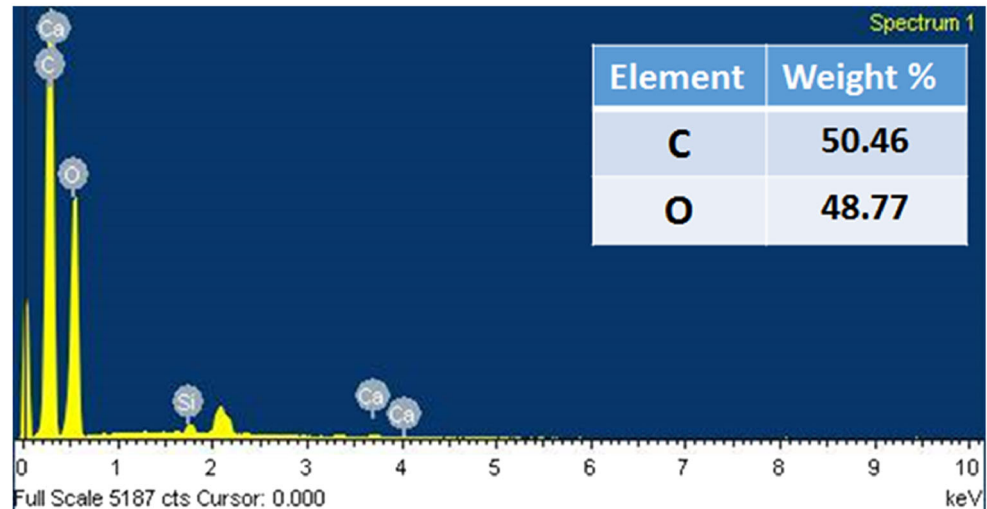


Fig. 2 b Stacking of sieves in descending order (b) Particle size distribution of bamboo filler

Fig. 3 a Optical micrograph of bamboo filler (b) EDS diagram of bamboo filler



(a)



(b)

For the quantification of improvement in the thermal stability of alkali treated filler as compared to untreated one, thermo gravimetric analysis (TGA) of both fillers is recorded from a thermal analyzer, STA 449 F3 Jupiter by conducting the test from room temperature to 800 °C at a heating rate of 10 °C/min under nitrogen atmosphere to create inert medium.

Fracture property test

The plane strain fracture toughness test of nominal brittle material ‘bamboo-epoxy composite’ samples are carried out in accordance with ASTM D 5045–14 with single edge notch

bending (SENB) specimen having dimension of 55 mm × 12.5 mm × 6.25 mm at the crosshead speed of 10 mm/min using universal testing machine (UTM) of test loads up to 50 kN. The schematic diagram of single edge notch bending (SENB) specimen is shown in Fig. 5. Toughness, being the one among important mechanical properties is calculated in terms of critical stress intensity factor (K_{Ic}) that measures the strength of stress singularity present at crack tip [25].

The value of plane strain fracture toughness (K_{Ic}) has been calculated using the expression (2) as follows.

$$K_{Ic} = \frac{P_Q}{BW^{0.5}} f(x), f(x) = 6x^{0.5} \frac{[1.99 - x(1-x)(2.15 - 3.93x + 2.7x^2)]}{(1+2x)(1-x)^{1.5}} \quad (2)$$

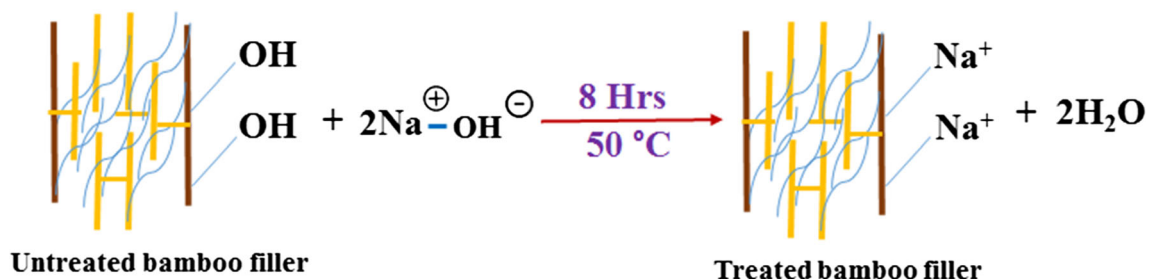


Fig. 4 Chemical reaction mechanism for surface modification of bamboo filler

Table 1 Weight loss of bamboo filler after alkaline treatment

Weight		% loss
Untreated filler	Treated filler	
8 g	5.14 g	35.75%

Where P_Q =Load, B =Specimen width, W =Specimen depth, $0 < x < 1$.

On the other hand, the fracture energy values (G_{Ic}) is calculated using following Eq. (3) written below.

$$G_{Ic} = \frac{U}{BW\phi}, \phi = \frac{18.64 + A}{dA/dx} \tag{3}$$

Where

$$A = [16x^2/(1-x)^2] [8.9-33.717x + 79.616x^2-112.952x^3 + 84.815x^4-25.672x^5]$$

$$dA/dx = [16x^2/(1-x)^2] [-33.717 + 159.232x-338.856x^2 + 339.26x^3-128.36x^4]$$

$$+ [32x/(1-x)^3] [8.9-33.717x + 79.616x^2-112.952x^3 + 84.815x^4-25.672x^5]$$

Total fifteen (15) number of composite specimens are tested and three for each filler content samples to ensure repeatability. The values representing the Mode I fracture toughness (K_{Ic}) and fracture energy (G_{Ic}) are taken an average from the result of testing three samples from different lots. The results obtained according to above-described method are considered to be valid if following criterion is met.

$$B, a, (W-a) > 2.5(K_{Ic}/\sigma_y)^2 \tag{4}$$

Where K_Q - Conditional K_{Ic} value, σ_y - Yield stress of the material, a - Crack length

Morphological observation

The morphology of prepared composite samples has been assessed using scanning electron microscopy (SEM) operating at 20 kV to evaluate the filler dispersion and its adherence

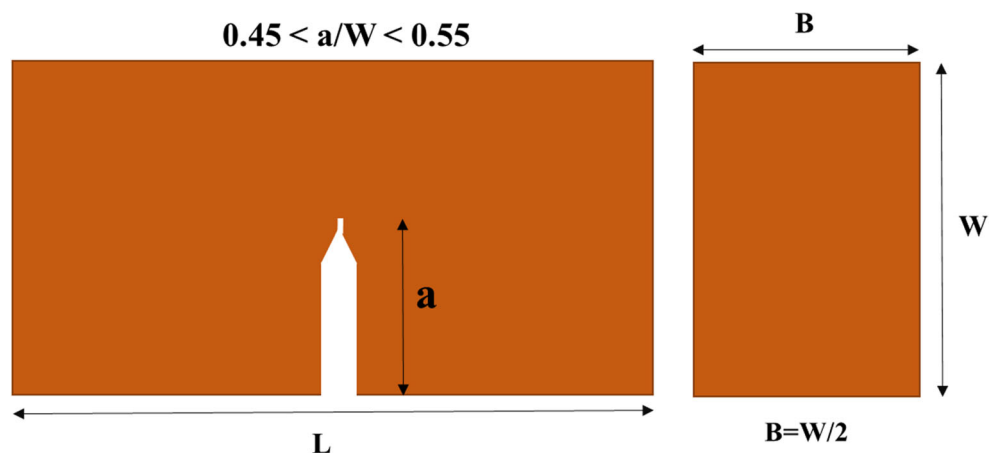
to the matrix. In addition, the fracture surface of composite samples are also analyzed to investigate about filler pullout and crack development. The samples are previously coated with platinum to avoid charging under the electron beam and viewed perpendicularly.

Results and discussions

Fourier transform infrared (FTIR) spectra

The FTIR spectral analysis of untreated and treated bamboo filler is carried out in Attenuated Total Reflection (ATR) mode for the functional group analysis and corresponding graph is presented in Fig. 6a, b respectively. Clear differences with respect to characteristic and location of bands can be visualized in treated and pristine fillers. The absence and reduction in transmittance and vibrational energy of moieties present in filler molecules can be clearly observed in case of treated bamboo fillers. The reduced intensity around wave number 3200–3300 cm^{-1} might be due to the removal of hydroxyl groups (-OH) from untreated filler surface owing to the alkali treatment [26]. The peaks around 2880–2899 cm^{-1} point to the presence of alkane compounds and decreased transmittance in case of treated filler revealing that the concentration of methylene group (-CH₂-) or methyne group (-CH<) is reduced. The alkali treatment results to significant difference in fibre structure. The surface of the fibre was covered with layers of substances like pectin, lignin and impurities. After alkali treatment along with hemicellulose component, pectin and lignin got removed from the fibre which was reflected in the infrared spectroscopy. The broad absorption band observed in 3415 cm^{-1} was related to hydrogen bonding (-OH) stretching vibration. This peak append weaker in intensity once it is treated with alkali. The vibration peak around 2899–2912 cm^{-1} , corresponding to the stretching of - C - H aliphatic group decreases after alkali treatment

Fig. 5 Schematic diagram of single edge notch bend (SENB) specimen



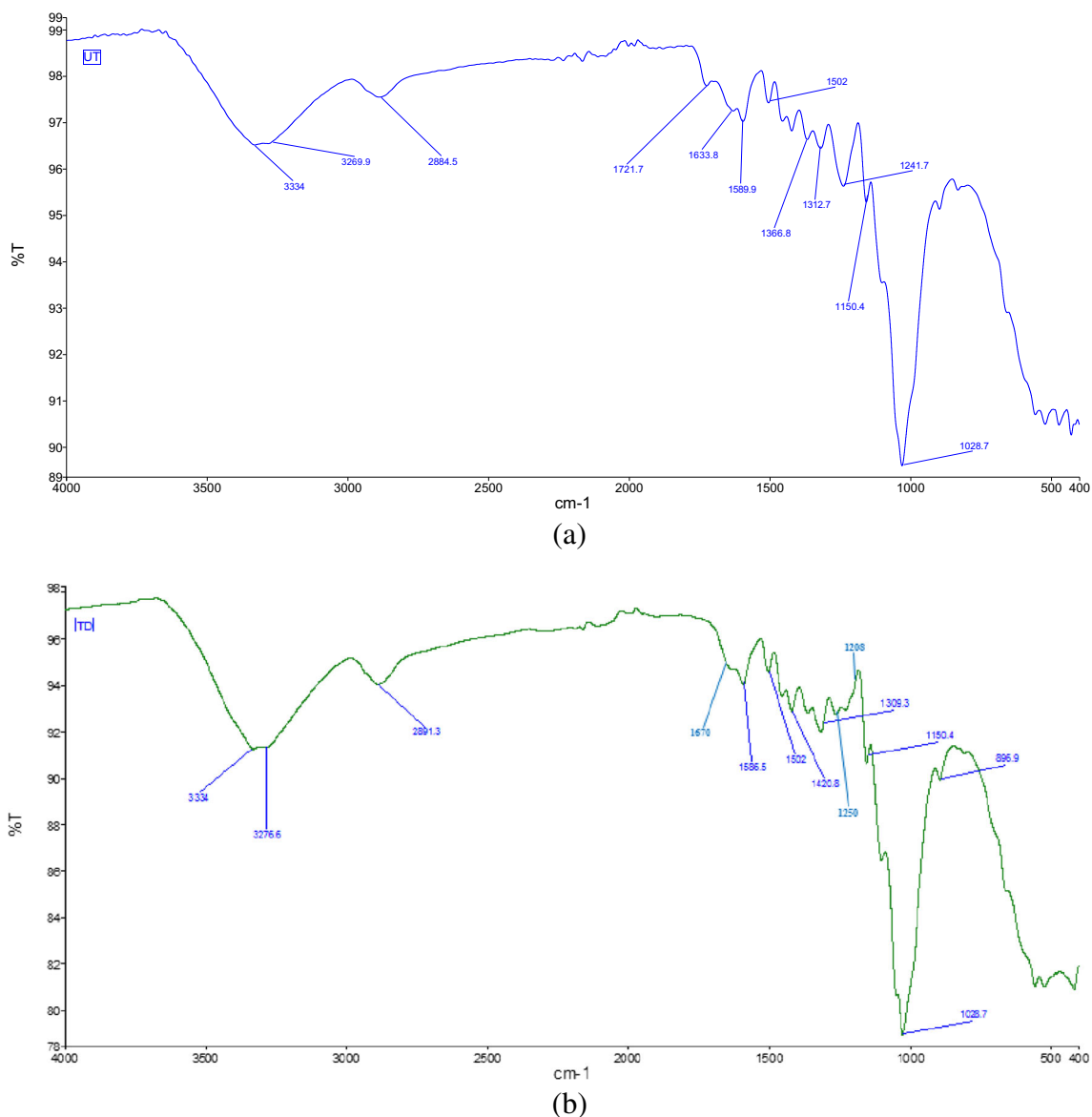


Fig. 6 FTIR spectra of (a) untreated and (b) treated bamboo filler in Attenuated total reflection (ATR) mode

due to removal of hemicellulose component. The characteristic peaks between 1800 and 1600 cm⁻¹ signify the carbonyl group (-C=O) and carboxylic groups (-COOH). Moreover the reduction in the molar ratio of hydrogen and oxygen as a result of alkaline treatment caused by lowering of the polarity of treated filler molecules. The downward shift of infrared spectra of treated filler is associated with the low energy excitations of the condensed aromatic groups which is very much common in plant-based bio fibrous material. The absorption peak for C=O stretch of acetyl group of lignin for untreated filler appears at 1721.7 cm⁻¹, and that for the treated filler is at 1670 cm⁻¹. This was due to the removal of lignin from fibre surface after surface treatment. This may also be due to the fact that alkali treatment removed the less polar hemicellulose and lignin component which increased the

overall polarity of the sample. The assessment of FTIR peaks is also presented in Table 2.

X-ray diffraction (XRD) analysis

The XRD analysis can directly provide structural along with crystal information and therefore commonly used in identifying various materials. The diffractogram of pristine and alkali treated bamboo filler is depicted in Fig. 7. It can be observed from the graph that the surface treatment through aqueous NaOH did bring a considerable increase in crystallinity of treated filler relative to the untreated counterpart. However, the substantial increase in crystalline region after treatment might be attributed to the partial removal of lignin and hemicellulose after reaction with sodium hydroxide molecules in form of reddish liquid [27]. Besides, the revised molecular

Table 2 Peak assessment of FTIR-ATR graph

Filler type	Hydroxyl group	Alkane compound group	Carbonyl group	Acetyl group
Untreated filler	3269.9 and 3334	2884.5	1721.7	1241.7
Treated filler	3276.6 and 3334	2891.3	1670	1250 and 1208

structure of treated filler can be better understood with the comparison between degree of crystallinity along with identification and placement of crystal planes before and after the treatment [28]. Both of these diffractogram contain one main peak corresponding to 22.3° and two shoulder peaks around 16° and 35°. Furthermore, the removal of -OH groups due to the elimination of lignin and other noncellulosic molecules has forced the reorganization of carboxylic and carbohydrate groups, resulting in the change of crystallinity index. The crystallinity index, a quantitative indicator of crystallinity is defined as the volume fraction of crystallinity of one phase in a given sample [29]. The extent of increase in the crystalline region at the expense of reduction in the amorphous region is calculated by the following equation by considering the XRD peak height method given Segal et al. [30]. The crystallinity index (I_c) and percentage of crystallinity of treated and untreated bamboo filler are calculated by following Eqs. 5 and 6.

$$\text{Crystallinity index } (I_c) = \frac{I'_{002} - I'_{am}}{I'_{002}} \tag{5}$$

$$\% \text{crystallinity} = \frac{I'_{002}}{(I'_{002} + I'_{am})} \times 100 \tag{6}$$

Where I_{002} - Maximum intensity of (0 0 2) crystal plane, I_{am} - Maximum intensity of the amorphous phase at $2\theta = 18^\circ$.

I'_{002} (true maximum intensity of (0 0 2) crystal plane after subtraction of the contribution due to the amorphous phase) = $I_{002} - I_{am}$, I'_{am} (true maximum intensity of the amorphous phase at 2 theta equals to 18 degrees after baseline correction) = $I_{am} - I_{baseline}$.

The calculated % crystallinity in the untreated filler is around 64.99%, whereas the same for treated filler is approximately 85.41%. On the other hand, crystallinity index for treated and untreated filler is found to be 0.83 and 0.46 respectively. It shows the effect of alkaline treatment on the crystal structure of bamboo filler. These crystallinity data are presented in Table 3. The various crystal planes present in the pristine and treated filler are (1 1 0) and (0 0 2) as also reported in previous work [31]. The distance between the (1 1 0) and (0 0 2) peak in the pristine filler is 6.72° whereas the distance between the same for treated filler is 5.82°. The two theta (2θ) value of full width at half maximum (FWHM) for treated and pristine bamboo filler is 3.46° and 4.57° respectively. Moreover, the alkali treatment also resulted in the molecular rearrangement of the initial atomic structure of untreated filler and even so formed a more thermally stable substance that is evident from thermogravimetric analysis of both fillers. The d-spacing of the two aforementioned crystal planes is calculated for both treated and untreated bamboo filler is presented in Table 4. The alkali treatment has affected the d-spacing of various planes.

Fig. 7 X-ray diffractogram of treated and untreated bamboo filler

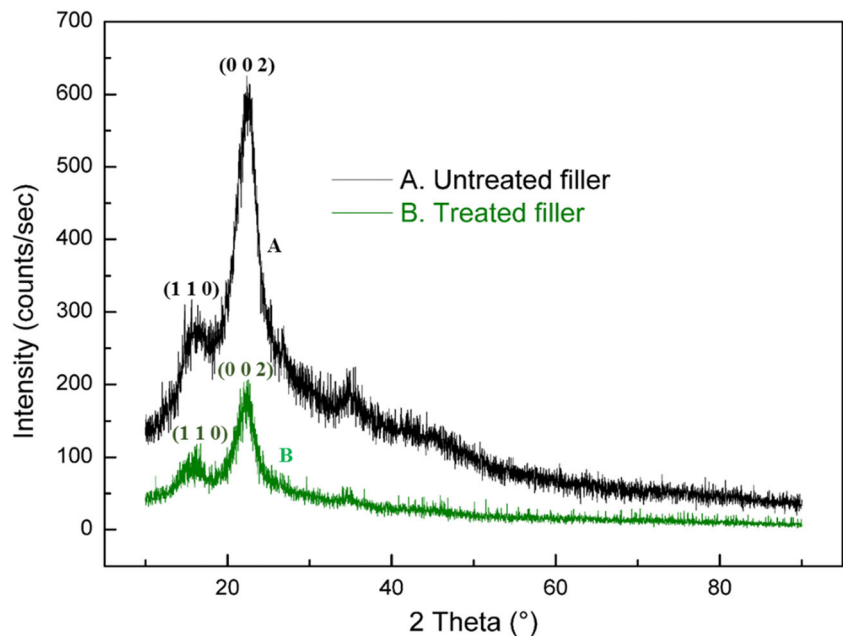


Table 3 Crystallinity percentage and crystallinity index of raw and treated bamboo filler

Filler type	I_{002}	I_{am}	$I_{baseline}$	Γ_{002}	Γ_{am}	Crystallinity index	Crystallinity %
Treated filler	186.15	61.33	40	124.82	21.33	0.83	84.51
Untreated filler	542	271	125	271	146	0.46	64.99

Thermogravimetric analysis (TGA)

The practical importance of thermal behaviour is concerned with the temperature rise above the ambient in unsolicited circumstances like fire damage or forced situation like heating and curing process. Considering this, thermogravimetric analysis has been carried out and the corresponding thermogram (TG) along with its first derivative (DTG) for untreated and treated bamboo filler are articulated in Figs. 8 and 9 respectively. The worth observing point is the three-stage degradation phenomenon owing to the decomposition of various constituents at different temperature range for both the pristine and treated filler as the temperature increases from ambient to 800 °C [18, 32]. The first stage of degradation for untreated filler took place from 26 °C to 237 °C and associated with the evaporation of moisture content/water molecules and elimination of light weight volatiles present in the molecular structure [33]. The second phase of decomposition which started at 237 °C and continued till 359 °C, is attributed to the cleavage of first cellulosic, then hemicellulosic and at last lignin part of filler molecules. For treated bamboo filler, the first phase of degradation occurred between 26 °C to 251 °C. Up to 100–150 °C, the constituent water molecules gets eliminated and further increasing temperature to 251 °C resulted in 8% of filler weight loss. Moreover the major weight loss (from 17 to 60%) process ended at temperature 374 °C which is about 15 °C higher than the same for untreated one. The three stages of weight loss are associated with both treated and untreated filler, the first stage up to °C corresponds to 10–17% of weight loss, and subsequent second stage up to 350 to 375 °C depicts a weight loss of approx. 60%. This one is followed by the last stage of decomposition extending up to 800 °C demonstrates remaining weight loss and formation of residual mass. Several parametric values like T_{Onset} , T_{50} and residual mass for pristine and treated bamboo fillers are presented in Table 5. The onset of major weight loss (obtained by the intersection of two tangent lines to the thermogram curve) also occurs a slightly higher temperature than the same for pristine filler as can be

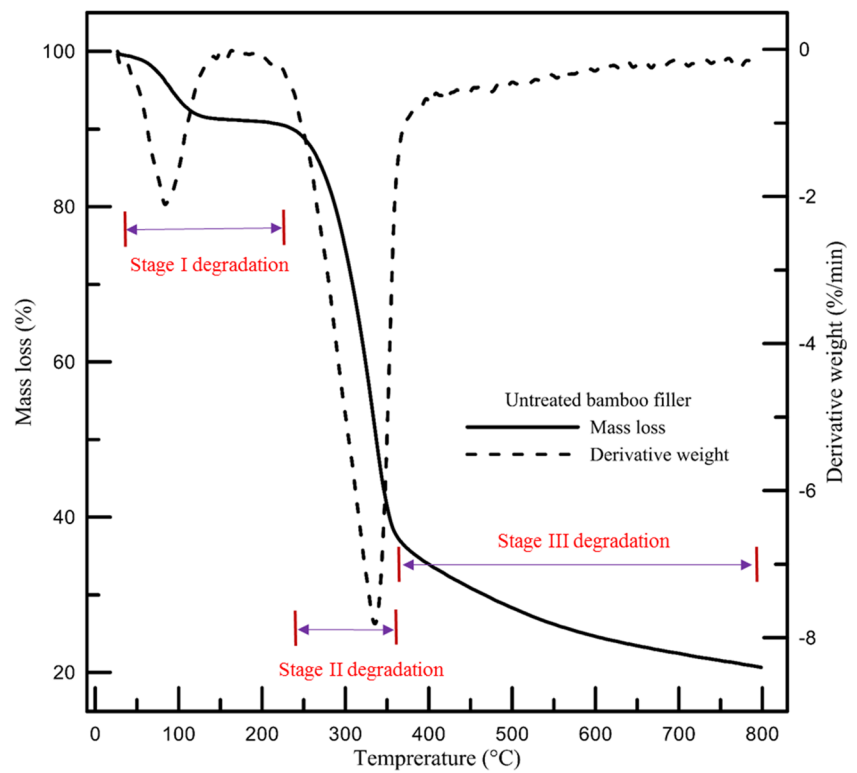
Table 4 d-spacing of crystal planes of raw and treated bamboo filler

Filler type	d-spacing of crystal planes (Angstrom)	
	(1 1 0)	(0 0 2)
Treated filler	2.6756	1.9992
Untreated filler	2.8625	2.0276

observed in Table 5. A comparison of two thermograms showed that the thermal stability of treated filler has been improved to a significant extent as a result of alkaline treatment. The residue (or ash content) leftover at the end of complete degradation is approx. 23% for treated filler while the same in case of pristine filler is 20%. The ashes (part of the filler corresponding to the inert material) amount remaining does not seem to be changing significantly after 600 °C to the end temperature of 800 °C [34]. The remaining weight at the end of the last leg of degradation represents the char or other products obtained from decomposition reaction. As the temperature is increased, the residual mass is decreased and also exhibit greater oxidative stability. The values obtained from the thermogravimetric analysis for treated and untreated filler in the present work is quite expected and similar values are reported for other natural bio fillers [32, 35].

The enhanced thermal stability in case of treated filler is connected with the covalent bonding of sodium ions (Na^+) onto filler molecules as shown in Fig. 3. Due to the graft copolymerization the hydroxyl group and other hydrophilic functional groups are replaced by sodium grafted ionic groups consequently improving the thermal stability of treated filler [36]. The observations made from thermograms are also supported by DTG curves. The DTG curve displays the maximum rate of thermal decomposition peak along with two upside-down shoulder and tail peaks corresponding to the filler materials constituents. The two points of inflexion can be observed for both the treated and untreated filler. The first point of inflexion for both the treated and untreated fillers are 84.3 °C and 83.9 °C respectively whereas the second point is at 352.7 °C and 335.4 °C. The presence of these two sharp upsides down peaks might be attributed to the dissociation of lignin and hemicellulose molecular chains. Initial sharp upside down peak of DTG curve signifies the water loss peak and inferred around 83–84 °C. The main DTG peak for both the filler occurs between 330 to 360 °C. It clearly shows the some effects of chemical treatment on maximum degradation rate temperature (MRDT). Moreover, the decomposition behaviour of both the modified and pristine filler observed to be similar in TG variation with a minor difference in DTG curvature around 300–340 °C. As a final remark, the effect of alkaline treatment to some extent succeeded in increasing the thermal stability of bamboo-based filler materials. Therefore for bamboo filler, a temperature limit of 280 °C might be considered as the working environment for its commercial application and reinforcing in various polymer matrices.

Fig. 8 Thermogravimetric analysis of untreated bamboo filler



Fracture properties

The fracture properties like fracture toughness and fracture energy are of high practical importance material attributes owing to the consideration of preexisted defects in the material

and existence of flaws cannot be completely ruled out during fabrication, processing and service of materials. The toughness represents materials resistance to fracture while strength is a function of the materials resistance to deformation [25]. There is a common practice to assume that the flaws (or

Fig. 9 Thermogravimetric analysis of treated bamboo filler

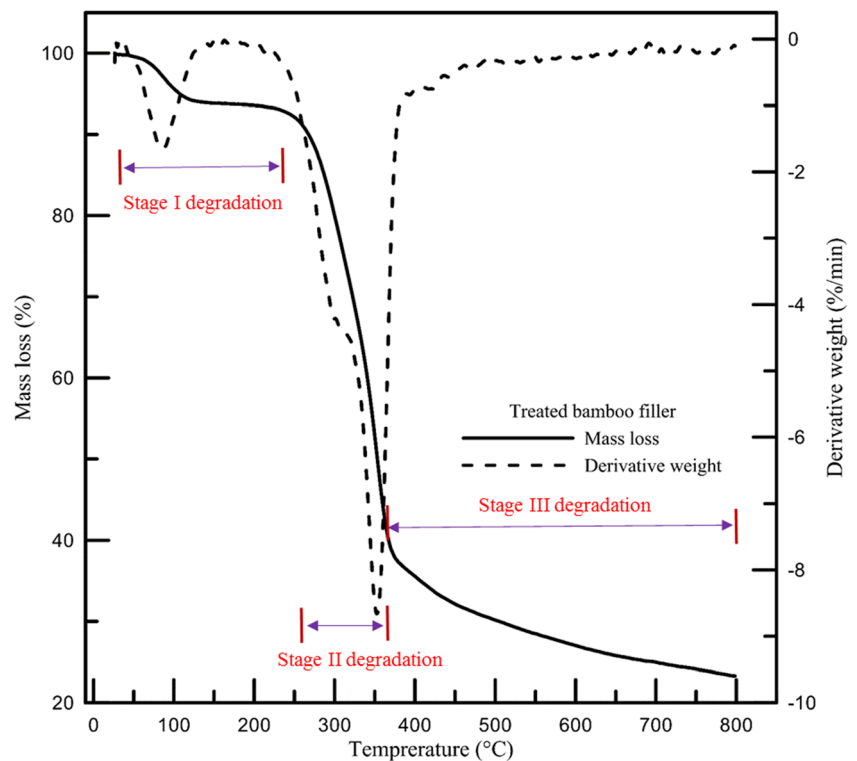


Table 5 Thermogravimetric analysis of untreated and treated bamboo filler

Filler type	IDT (T_{onset})	MRDT	T_{50}	Final residue
Treated filler	72.8 °C	352.7 °C	352.5 °C	23.29%
Untreated filler	67.8 °C	335.4 °C	336.7 °C	20.64%

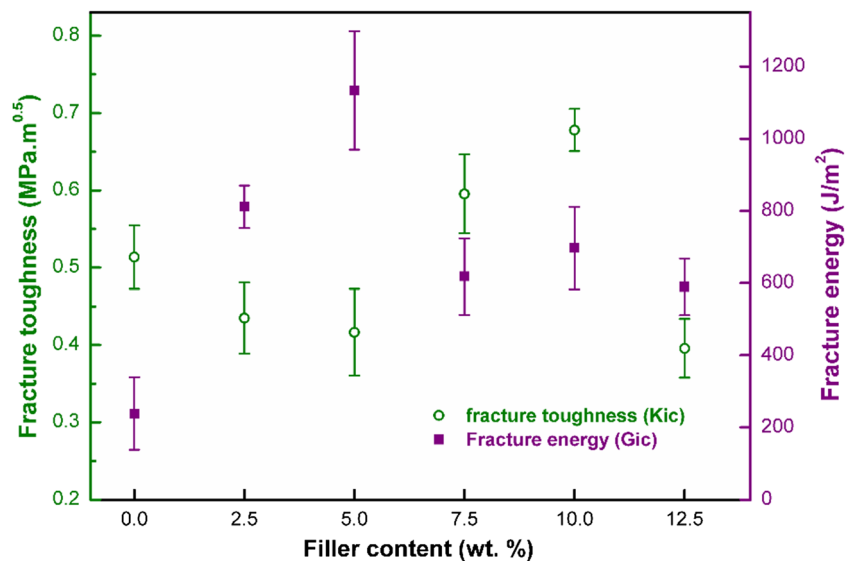
cracks) of some known size will already be present in the material and utilize linear elastic fracture mechanics (LEFM) to design the machine components. Mode I type of fracture failure has occurred in all of the specimens due to the presence of tensile stress normal to the plane of crack. The fracture toughness (K_{Ic}) and fracture energy (G_{Ic}) values for bamboo-epoxy composite samples together with the neat epoxy specimen is demonstrated in Fig. 10. The error bars here indicate the maximum and minimum values.

The K_{Ic} value for a composite sample of filler loading 2.5 wt.% is $0.435 \text{ MPa}\cdot\text{m}^{0.5}$ which is approximately 38% lower than the same for neat epoxy samples. The neat epoxy samples exhibited the fracture toughness value of $0.51 \text{ MPa}\cdot\text{m}^{0.5}$. Increasing the filler amount to 5% has further decreased the fracture toughness values to $0.4164 \text{ MPa}\cdot\text{m}^{0.5}$. However, this decreasing trend has been reversed with filler addition of 7.5% and the fracture toughness values has been enhanced to $0.5954 \text{ MPa}\cdot\text{m}^{0.5}$. The significant improvement in fracture toughness values might be associated with the obstructions produced in the propagating path of crack fronts with the presence of bamboo filler particles. The obstacles have delayed the failure occurrence time and the samples sustain a greater amount of applied load [37]. The increasing amount of filler content to 10 wt.% has significantly improved the plane strain fracture toughness to $0.6781 \text{ MPa}\cdot\text{m}^{0.5}$ but the rate of increment drops in comparison to the increase in filler inclusion. Moreover, the reinforcement of 12.5 wt.% has

adversely affected the toughness values as 42% drop as comparison to previous value, can be observed. The reason attached to this expected behaviour is weaker bonding between filler particles and matrix, resulting in easier crack penetration through the interface. The findings are in line with the earlier reported works on wood and coir filler composites [19, 35, 38, and]. The material response in terms of stress-strain variation for bamboo-epoxy composite sample can be observed from Fig. 11 for better understanding of its design aspect.

On the other hand, fracture energy (G_{Ic}) values observed to be increased up to 5 wt.% of filler content and beyond that an almost unfilling drop has been found. The G_{Ic} value for the base matrix is 239 J/m^2 whereas among composite samples, maximum value of fracture energy is 1134 J/m^2 . It can be observed that the addition of bamboo micron fillers has considerably enhanced the fracture energy values roughly by 3 to 5 times (from 590 to 1134 J/m^2) as compared with neat epoxy value. The detected increase in strain energy release rate for some filler loading might be linked to the toughening effect of bamboo fillers when added to the base polymer. The lowest fracture energy is depicted for 12.5 wt.% of filler content, but still the observed value is higher than the neat polymer samples. The observed value range of fracture energy in the present work is significantly higher than the same for glass particle reinforced epoxy composite material as reported in previous investigations [37]. The fracture properties of bamboo-epoxy composite is compared with existing different natural filler/synthetic filler based polymer composite material as presented in Table 6.

The wood filler and coir filler based epoxy composites demonstrated the lower value range for fracture energy but higher value in case of fracture toughness [19, 35]. Moreover, the fracture energy of carbon nano bead reinforced epoxy composite material is found to be around half of the same for bamboo-epoxy composite samples. Another worth

Fig. 10 Fracture properties of bamboo-epoxy composite

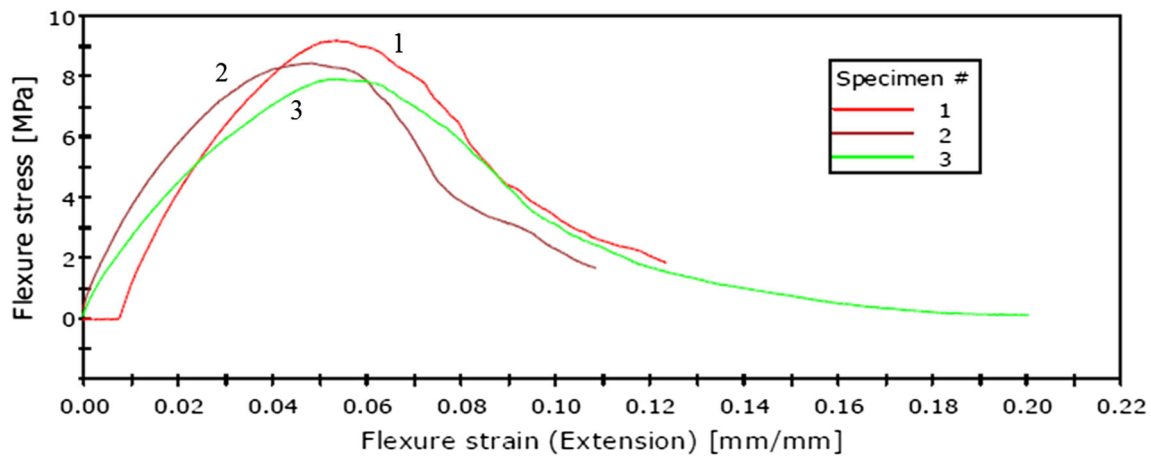


Fig. 11 Stress vs. strain in 3-point loading of SENB specimen

discussing point is the practical importance of these fracture results [39]. In industrial terms, these results mean that traditional materials used in shoe sole, ankle foot orthosis (AFO) and in other like applications can be replaced with the developed bamboo-epoxy composites. Moreover, the drop in G_{Ic} values from filler loading of 7.5 wt.% and onwards is interconnected to the agglomerated and clustered filler particles, high debondability with matrix thus ensuing the relatively higher penetration of cracks across the particle array. The schematic diagram of 3-point bending load of composite samples is demonstrated in Fig. 12a, b respectively for low and high filler contents. The crack propagation line and obstructions confronted by the crack tip due to the presence of filler particles can be observed. The penetration of cracks through the material interfaces in presence of binary phase (solid bamboo filler and epoxy matrix) has been governed by following fracture mechanisms.

Crack front twisting

The presence of weakly bonded secondary phase has instigated the seamless propagation of crack front consequently twisting of its tip until it attains the maximum angle of twist (Φ) as shown in Fig. 13a. The crack propagation leaves tail lines between the bamboo filler particle that came across which signifies its direction. This creates an additional surface area for crack propagation and extra dissipation of energy took

place, therefore, more weakening of filler-matrix interface [40]. This type of fracture mechanism is mostly applicable to low filler content samples like 2.5% and 5%. At a low amount of filler loading, the separation of consecutive particles is greater thus the crack mostly travels through the matrix phase and also reducing the maximum twist angle.

Crack tip bowing

The crack tip bowing occurs as a result of the meeting of primary cracks with particles and impeded by the encountered particles resulting in bowing of crack front between consecutive particles as depicted in Fig. 13b. The bowing crack (also known as ‘secondary cracks’) bypasses the impenetrable particles and interacting with neighboring cracks when its shape becomes semicircular [41]. The crack tip remains bowed state under stress in form of a nonlinear crack front as long as the particles bridge the crack. The stress intensity factor (K_{Ic}) decreases along the bowing section and moreover, a higher energy is required to increase toughness.

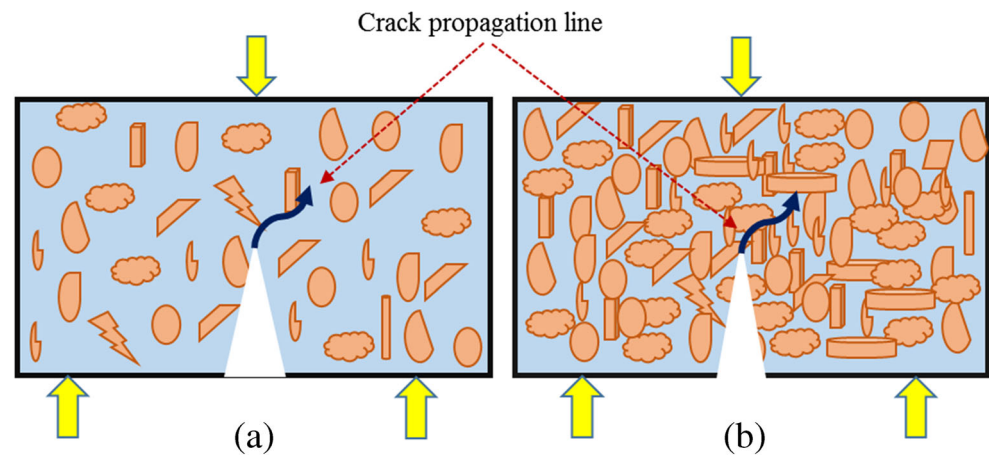
Crack pinning

The impenetrable obstacles in form of bamboo particle fillers have been instrumental in blocking or deflecting the crack path, consequently resulted in kneeling of the primary crack between the particles. This has led to formation of secondary

Table 6 Comparison of fracture properties of bamboo-epoxy composite with other existing natural filler/synthetic filler based polymer composites

Reported works	Composite type/Neat epoxy	Filler content	Fracture toughness (MPa.m ^{0.5})	Fracture energy (J/m ²)
Kumar et al. 2018	Wood filler epoxy composite	10 wt.%	0.553	717.77
Kumar et al. 2017	Coir filler epoxy composite	5 wt.%	1.792	970.46
Goyat et al. 2015	Carbon nano bead-epoxy composite	2 wt.%	0.79	545
Present research work	Neat epoxy	0 wt.%	0.51	239
	Bamboo-epoxy composite	10 wt.%	0.678	1133.89

Fig. 12 Fracture sample loading diagram and crack propagation line



cracks that is pinned at the encountering places of several particles present in the row [42]. The crack pinning mechanism is demonstrated in Fig. 13c. The secondary crack length is initially small but as propagates the length enlarges due to the change in shape of the crack between the pinned positions. This fracture mechanism is responsible for enhancement in toughness values for particle reinforced composites.

Crack front blunting

The crack pinning is followed by blunting of propagating crack fronts as depicted in Fig. 13d. The associated reason for this phenomenon is localized shear yielding at the tip of the crack front that resulted in destabilizing (like stick/slip) the crack propagation. Here the crack growth is retarded owing to the debonding of filler particles [43]. The mechanism of fracture happening like this is expected to take place for high filler loading samples like 10% and 12.5%. The formation of delamination induced crack perpendicular to a notch front acts as initiators for blunting process. The tortuous route of crack propagation represents the unique style of blunting mechanism.

Crack tip shielding

The crack tip shielding effect is highly dependent on particle size and its location. Larger the particle size, greater is the chance of crack tip shielding. The crack shielding behaviour reflects the actual level of plastic deformation associated with the crack growth and also decreases the rate of crack growth. The shielding of crack tip induces the transformation of particles dispersed at the crack tip and developed a residual strain fields [44]. This has been resulted in enhanced fracture toughness value and reduction in effective crack driving force. This fracture mechanism arises as a consequence of plasticity generated both at the crack tip and along the crack flanks of propagation line.

Morphological observation

The dispersion of the reinforced bamboo filler in the epoxy polymer matrix is assessed and the observed morphological images have been depicted in Fig. 14a–c respectively for 5%, 7.5% and 12.5% of filler content. As shown, the fillers are dispersed discretely as well as homogeneously and appeared separately

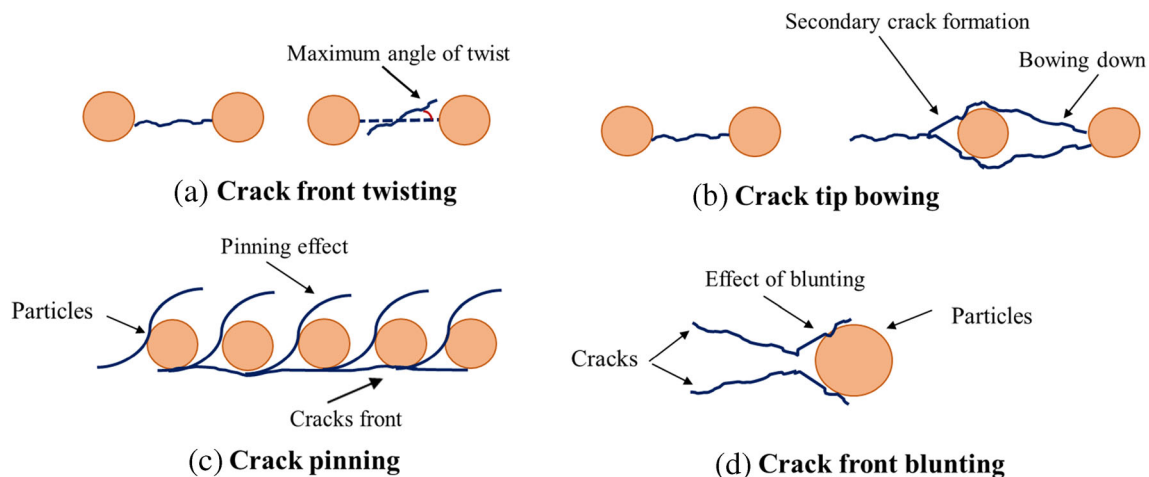


Fig. 13 Different fracture mechanisms in particle reinforced composites

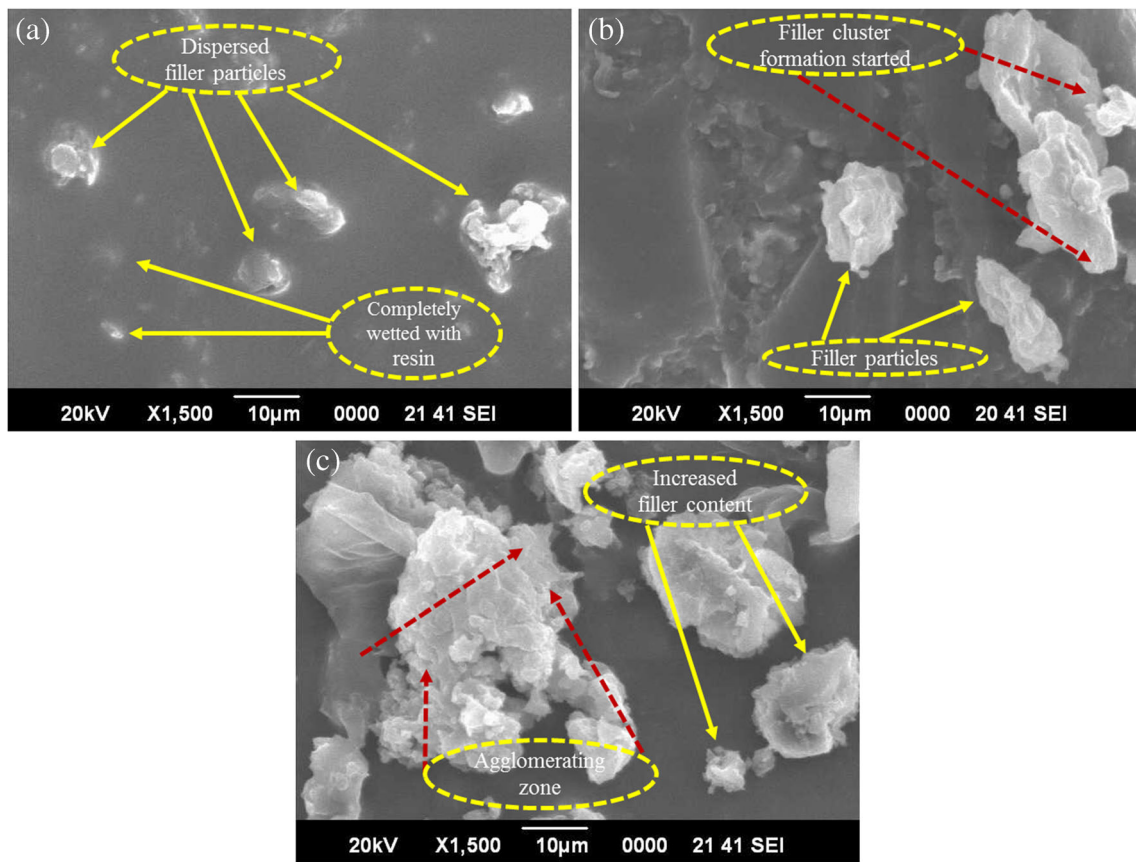


Fig. 14 Scanning electron micrographs (SEM) of composite samples of (a) 5% (b) 7.5% (c) 12.5%

without overlapping each other in Fig. 14a. A two-phase microstructure is present and shows good wetting of fillers with a layer of matrix resin covering it. Therefore the fibrillar interaction between filler to filler and filler to matrix looks like excellent, which converted into better fracture properties. Furthermore, the included filler loading of 7.5% caused a significant increase in population density of filler particles for a given matrix volume, thus creating assemblage and cluster formation of fillers. This can be evidently observed from Fig. 14b as yellow dotted circles and directed by red arrows. At this stage, the fracture toughness

value is increased but a drop is observed in fracture energy values. Meanwhile, the further filler addition displayed a more congested, irregularly distributed and piling-up of fillers at several places in the microstructure as depicted in Fig. 14c. The accumulation of filler particles might have diminished the obvious interaction of filler-matrix and resulted in adversely affecting the composite properties as validated from fracture properties drop at aforementioned filler loading [45]. At this filler content, the fracture toughness as well as fracture energy values found to be the lowest among composite samples. In addition, the

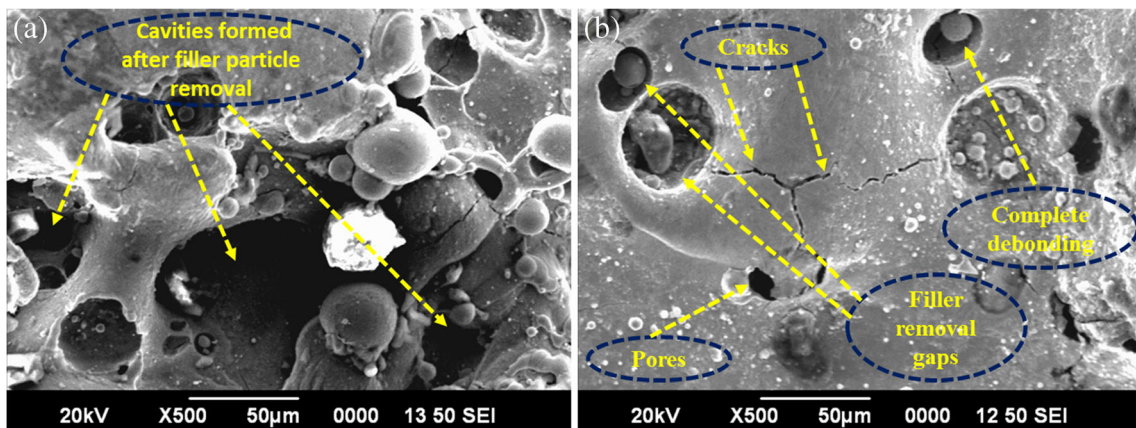


Fig. 15 SEM images of fracture surface of SENB specimen

perceived filler clusters entrapped the resin and suppressed the full-fledged bonding to be developed between matrix and filler. Also matrix infiltration and wetting became difficult which could have been prevented at the lower reinforcing amount of fillers.

The SEM images of the fractured surface of composite samples after the fracture test are described in Fig. 15a, b. The debonding and cavities formed due to pull out of bamboo fillers with and from the epoxy matrix can be apparently noticed. The clear phase separation of aggregated fillers from matrix took place as a result of pull out. However, the adhesive bonding between filler and matrix looks good at some places as shown in Fig. 15a. Nonetheless, the poor wetting of fillers and residuals of matrix material can also be observed in Fig. 15b owing to greater filler amount. The macro pores can also be seen at the wrecked surface of composite samples. These pores (or voids) might be the potential source for crack initiation and its rapid propagation. The formation of pores is associated with the two reasons, first one is related to the trapping of air bubbles in the mould during pouring of the filler-matrix mixture and other one being an inability of matrix resin to reach out the each and every place in the casting mould.

Conclusion and remarks

The present work has been carried out on the utilization of bamboo particle fillers of ‘micron size range’ in the production of eco-friendly epoxy based polymer composite material. The following conclusions can be deduced from the described research work.

- The bamboo fillers are prepared from bamboo culms by extracting, cutting, soaking and eventually grinding in a ball mill to reduce to the desired micron size. The utilized methodology for filler preparation can be applied to produce size range from ‘micron to nano’ in future works.
- The effectiveness of alkali treatment apparently reduces (or to some extent removes) the hydroxyl groups from filler molecules as evident from infrared spectra and thermogravimetric analysis. The percentage of lignin and other hemicellulosic material removal is around 35.75% as obtained from the weight loss of bamboo filler after treatment.
- The crystallinity index and percentage of crystallinity of bamboo filler has been increased by about 0.37 and 19.5% after the alkaline treatment respectively. Therefore, it appears that aqueous NaOH solution of 5% (w/v) is quite effective in enhancing the crystalline region in filler molecular structure.
- The thermal stability of treated filler seems to be enhanced by merely 3% with respect to the untreated counterpart in terms of residual mass at the end of degradation. The difference between T_{Onset} of treated and untreated filler is 5 °C, first one being the

72.8 °C. The thermal decomposition of both the fillers has followed the three step degradation process and demonstrates the two points of inflection.

- The fracture toughness value is found to be increased by 21% as compared to virgin epoxy samples through the inclusion of treated bamboo filler and the maximum value is 0.678 MPa.m^{0.5}. The found fracture toughness value is substantial and signifies the industrial application of the developed material in shoe soles and ankle-foot orthosis (AFO) of patients struggling with foot drop problem.
- The bamboo filler endowed significant gain in fracture properties of epoxy polymer and mechanisms concerned with fracture are crack pinning, crack front twisting and crack tip blunting respectively for lower and higher filler contents. These fracture mechanisms are principally applicable to micron size filler particles.

Nevertheless, the present research is confined to bamboo based micro-filler preparation and its application, the follow-up works might be focused on balancing strength-toughness property and further improvement in thermal stability of bamboo filler to employ in temperature sensitive applications. The major benefits of the developed bamboo-epoxy composite would be a relatively lower amount of filler content (up to 10%) where they have distinctive fracture properties as per existing natural bio-filler based plastic material.

Acknowledgements The authors would like to acknowledge SAIF-IIT Bombay and SAIC-Gauhati University for providing necessary technical assistances for FTIR and XRD. The authors also would like to thank Machine element laboratory and Material testing laboratory, MED, NIT Silchar for giving essential research facilities. The first author gratefully acknowledges the Ministry of Human Resource Development (MHRD), GOI for fellowship during his PhD work.

Compliance with ethical standards

Conflict of interest The author(s) declared no potential conflicts of interest with respect to the research, authorship, and/or publication of this article.

Publisher's note Springer Nature remains neutral with regard to jurisdictional claims in published maps and institutional affiliations.

References

1. Nagarajan V, Mohanty AK, Misra M (2016) Perspective on Polylactic acid (PLA) based sustainable materials for durable applications: focus on toughness and heat resistance. ACS Sustain Chem Eng 4:2899–2916
2. Gross RA, Kalra B (2002) Biodegradable polymers for the environment. Science 297(5582):803–807
3. Haque MM, Islam MS, Islam MN (2012) Preparation and characterization of polypropylene composites reinforced with chemically treated coir. J Polym Res 19(5):9847

4. Rahman MM, Netravali AN, Tiimob BJ, Rangari VK (2014) Bioderived “green” composite from soy protein and eggshell Nanopowder. *ACS Sustain Chem Eng* 2:2329–2337
5. Kumar R, Kumar K, Sahoo P, Bhowmik S (2014) Study of mechanical properties of wood dust reinforced epoxy composite. *Procedia Mater Sci* 6:551–556
6. Anand P, Rajesh D, Kumar MS, Raj IS (2018) Investigations on the performances of treated jute/Kenaf hybrid natural fiber reinforced epoxy composite. *J Polym Res* 25(4):94
7. Liu D, Song J, Anderson DP, Chang PR, Hua Y (2012) Bamboo fiber and its reinforced composites: structure and properties. *Cellulose* 19:1449–1480
8. Kumar R, Bhowmik S, Kumar K (2017) Establishment and effect of constraint on different mechanical properties of bamboo filler reinforced epoxy composite. *Int Polym Process* 32(3):308–315
9. Kabir MM, Wang H, Lau KT, Cardona F (2012) Chemical treatments on plant-based natural fibre reinforced polymer composites: an overview. *Compos Part B* 43:2883–2892
10. Li X, Tabil LG, Panigrahi S (2007) Chemical treatments of natural fiber for use in natural fiber-reinforced composites: a review. *J Polym Environ* 15:25–33
11. Kushwaha PK, Kumar R (2010) Bamboo fiber reinforced thermo-setting resin composites: effect of graft copolymerization of fiber with methacrylamide. *J Appl Polym Sci* 118:1006–1013
12. Nirmal U, Hashim J, Low KO (2012) Adhesive wear and frictional performance of bamboo fibres reinforced epoxy composite. *Tribol Int* 47:122–133
13. Yu Y, Huang X (2014) Yu W (2014) a novel process to improve yield and mechanical performance of bamboo fiber reinforced composite via mechanical treatments. *Compos Part B* 56:48–53
14. Khalil AHPS, Bhat IUH, Jawaid M, Zaidon A, Hermawan D (2012) Hadi YS (2012) bamboo fibre reinforced biocomposites: a review. *Mater Des* 42:353–368
15. Rajulu AV, Baksh SA, Reddy GR, Chary KN (1998) (1998) chemical resistance and tensile properties of short bamboo fibre reinforced epoxy composites. *J Reinf Plast Compos* 17: 1507–1511
16. Liu H, Wu Q, Han G, Yao F, Kojima Y, Suzuki S (2008) Compatibilizing and toughening bamboo flour-filled HDPE composites: mechanical properties and morphologies. *Compos Part A* 39:1891–1900
17. Zhou XX, Yu Y, Chen LH (2015) Effects of zirconaluminat coupling agent on mechanical properties, rheological behavior and thermal stability of bamboo powder/polypropylene foaming composites. *Eur J Wood Prod* 73:199–207
18. Thakur VK, Kessler MR (2014) Synthesis and characterization of AN-g-SOY for sustainable polymer composites. *ACS Sustain Chem Eng* 2(10):2454–2460
19. Kumar R, Kumar K, Bhowmik S (2017) Assessment and response of treated *Cocos nucifera* reinforced toughened epoxy composite towards fracture and viscoelastic properties. *J Polym Environ* 26:1–14. <https://doi.org/10.1007/s10924-017-1150-y>
20. Henke L, Zarrinbakhsh N, Endres HJ, Misra M, Mohanty AK (2017) Biodegradable and bio-based green blends from carbon dioxide-derived bioplastic and poly (butylene succinate). *J Polym Environ* 25(2):499–509
21. Nagarajan V, Mohanty AK, Misra M (2016b) Biocomposites with size-fractionated biocarbon: influence of the microstructure on macroscopic properties. *ACS Omega* 1(4):636–647
22. Dang W, Kubouchi M, Yamamoto S, Sembokuya H, Tsuda K (2002) An approach to chemical recycling of epoxy resin cured with amine using nitric acid. *Polymer* 43(10):2953–2958
23. Gorrasi G, Sorrentino A (2015) Mechanical milling as a technology to produce structural and functional bio-nanocomposites. *Green Chem* 17(5):2610–2625
24. Mishra S, Misra M, Tripathy SS, Nayak SK, Mohanty AK (2001) Graft copolymerization of acrylonitrile on chemically modified sisal fibers. *Macromol Mater Eng* 286:107–113
25. Shekhawat A, Ritchie RO (2016) Toughness and strength of nanocrystalline graphene. *Nat Commun* 7:10546
26. Behazin E, Misra M, Mohanty AK (2017) Sustainable biocarbon from pyrolyzed perennial grasses and their effects on impact modified polypropylene biocomposites. *Compos Part B* 118:116–124
27. Kafy A, Kim HC, Zhai L, Kim JW, Kang TJ (2017) Cellulose long fibers fabricated from cellulose nano fibers and its strong and tough characteristics. *Sci Rep* 7(1):17683
28. Nam S, French AD, Condon BD, Concha M (2016) Segal crystallinity index revisited by the simulation of X-ray diffraction patterns of cotton cellulose I β and cellulose II. *Carbohydr Polym* 135:1–9
29. French AD (2014) Idealized powder diffraction patterns for cellulose polymorphs. *Cellulose* 21(2):885–896
30. Sa Y, Guo Y, Feng X, Wang M, Li P, Gao Y, Yang X, Jiang T (2017) Are different crystallinity-index-calculating methods of hydroxyapatite efficient and consistent? *New J Chem* 41(13):5723–5731
31. Segal LGJMA, Creely JJ, Martin Jr AE, Conrad CM (1959) An empirical method for estimating the degree of crystallinity of native cellulose using the X-ray diffractometer. *Text Res J* 29(10):786–794
32. Abidi N, Cabrales L, Eric H (2010) Thermogravimetric analysis of developing cotton fibers. *Thermochim Acta* 498:27–32
33. Li Y, Jiang L, Xiong C, Peng W (2015) Effect of different surface treatment for bamboo Fiber on the crystallization behavior and mechanical property of bamboo Fiber/Nanohydroxyapatite/poly (lactico-glycolic) composite. *Ind Eng Chem Res* 54(48):12017–12024
34. Ferreira MVF, Neves ACC, de Oliveira CG, Lopes FPD, Margem FM, Vieira CMF, Monteiro SN (2017) Thermogravimetric characterization of polyester matrix composites reinforced with eucalyptus fibers. *J Mater Res Technol* 6(4):396–400
35. Kumar R, Kumar K, Bhowmik S (2018) Mechanical characterization and quantification of tensile, fracture and viscoelastic characteristics of wood filler reinforced epoxy composite, wood Sci. *Technol* 52(3):677–699
36. Monteiro SN, Calado V, Rodriguez RJS, Margem FM (2012) Thermogravimetric behavior of natural fibers reinforced polymer composites—an overview. *Mater Sci Eng A* 557:17–28
37. Spanoudakis J, Young RJ (1984) Crack propagation in a glass particle-filled epoxy resin. *J Mater Sci* 19(2):473–486
38. Wong KJ, Yousif BF, Low KO, Ng Y, Tan SL (2010) Effects of fillers on the fracture behaviour of particulate polyester composites. *J Strain Anal Eng Des* 45(1):67–78
39. Goyat MS, Suresh S, Bahl S, Halder S, Ghosh PK (2015) Thermomechanical response and toughening mechanisms of a carbon nano bead reinforced epoxy composite. *Mater Chem Phys* 166: 144–152
40. Singleton ACN, Baillie CA, Beaumont PWR, Peijs T (2003) On the mechanical properties, deformation and fracture of a natural fiber/ recycled polymer composite. *Compos Part B* 34(6):519–526
41. Li Y, Zhou Q, Zhang S, Huang P, Xu K, Wang F, Lu T (2018) On the role of weak interface in crack blunting process in nanoscale layered composites. *Appl Surf Sci* 433:957–962
42. Kitey R, Phan AV, Tippur HV, Kaplan T (2006) Modeling of crack growth through particulate clusters in brittle matrix by symmetric-Galerkin boundary element method. *Int J Fract* 141(1–2):11–25
43. Khan Z, Yousif BF, Islam M (2017) Fracture behaviour of bamboo fiber reinforced epoxy composites. *Compos Part B* 116:186–199
44. James MN, Christopher CJ, Lu Y, Patterson EA (2012) Fatigue crack growth and craze-induced crack tip shielding in polycarbonate. *Polymer* 53(7):1558–1570
45. Gope PC, Rao DK (2016) Fracture behaviour of epoxy biocomposite reinforced with short coconut fibres (*Cocos nucifera*) and walnut particles (*Juglans regia* L.). *J Thermoplast Compos Mater* 29(8):1098–1117